Supplementary Figures and Tables

Transfroming growth factor-β1 promotes lymphangiogenesis during peritoneal fibrosis

Hiroshi Kinashi[1], Yasuhiko Ito[1], Masashi Mizuno[1], Yasuhiro Suzuki[1], Takeshi Terabayashi[1],Fumiko Nagura[1], Ryohei Hattori[2], Yoshihisa Matsukawa[2], Tomohiro Mizuno[3], Yukihiro Noda[3], Hayato Nishimura[4], Ryosuke Nishio[5], Shoichi Maruyama[1], Enyu Imai[1], Seiichi Matsuo[1] and Yoshifumi Takei[6]

[1] Department of Nephrology and Renal Replacement Therapy and
[2]Department of Urology, Nagoya University Graduate School of Medicine, Nagoya, Japan,
[3] Division of Clinical Sciences and Neurosychopharmacology,
Meijyo University Graduate School of Medicine, Nagoya, Japan
[4]Department of Nephrology, Toyota Kosei Hospital, Toyota, Japan
[5]Department of Emergency Medicine, Kyoto University Hospital, Kyoto, Japan
[6]Department of Biochemistry, Nagoya University Graduate School of Medicine, Nagoya, Japan

Supplementary Figure 1. The number of lymphatic vessels and VEGF-C expression were increased in UFF-peritoneum compared to pre-dialysis uremia peritoneum.
Peritoneum was analyzed by immunohistochemistry. Lymphatic vessels were stained with an anti-LYVE-1 antibody. Blood vessels were stained with an anti-Pathologische Anatomie Leiden-Endothelium (PAL-E) antibody. Some mononuclear cells and non-vascular structures were revealed in immunostaining of LYVE-1 (D, G-J). These cells may be derived from other cells, such as macrophages, which may potentially transform to the lymphatic vessels (Ref. 1-3).
A and B: PAL-E, **C and D**: LYVE-1, **E and F**: VEGF-C, **G-J**: double staining of LYVE-1 (red) and PAL-E (blue). (**A, C and E**) and (**B, D and F**) were serial sections of the same patient. Scale bars, 200 μm.

References

1. El-Chemaly S, Malide D, Zudaire E, Ikeda Y, Weinberg BA, Pacheco-Rodriguez G, Rosas IO, Aparicio M, Ren P, MacDonald SD, Wu HP, Nathan SD, Cuttitta F, McCoy JP, Gochuico BR & Moss J: Abnormal lymphangiogenesis in idiopathic pulmonary fibrosis with insights into cellular and molecular mechanisms. Proc Natl Acad Sci U S A 106: 3958-3963, 2009
2. Maruyama K, Ii M, Cursiefen C, Jackson DG, Keino H, Tomita M, Van Rooijen N, Takenaka H, D'Amore PA, Stein-Streilein J, Losordo DW & Streilein JW: Inflammation-induced lymphangiogenesis in the cornea arises from CD11b-positive macrophages. J Clin Invest 115: 2363-2372, 2005
3. Kerjaschki D: The crucial role of macrophages in lymphangiogenesis. J Clin Invest 115: 2316–2319, 2005

Supplementary Figure 1

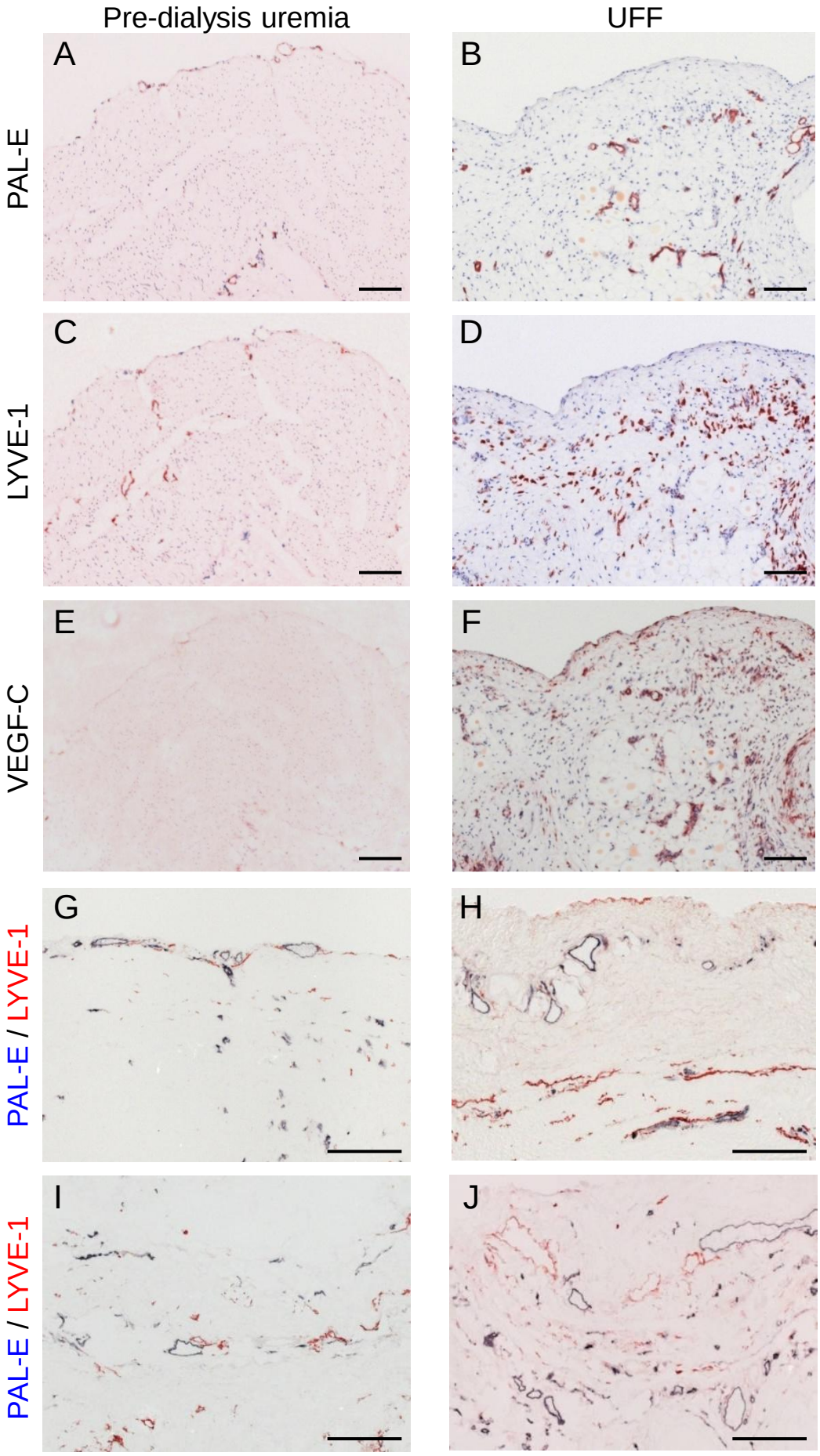

Supplementary Figure 1

Supplementary Figure 2.

Analysis of VEGF receptor-3 (VEGFR-3) expression in the diaphragm of control and CG model rats and in human peritoneal mesothelial cells and normal human lymphatic microvascular endothelial cells.

(A-E) Immunofluorescent staining of VEGFR-3 (green) in the diaphragms of representative control (**A and C**) and CG model (**B and D**) rats. Nuclei were counterstained with DAPI (blue). The level of VEGFR-3 expression, which was detected in the lymphatics, was increased in the CG model.
E: Double staining of VEGFR-3 and podoplanin in the diaphragm of a CG rat.
Scale bars, 200 μm.
F: RT-PCR analysis of the mRNA expression of VEGFR-3, in human peritoneal mesothelial cells (HPMC) from patients with high and low peritoneal transport, and in normal human lymphatic microvascular endothelial cells (HMVEC-LLy). GAPDH was used as a loading control. VEGFR-3 mRNA was only detected in HMVEC-LLy cells.

Methods
HMVEC-LLy cells were purchased from Lonza Bioscience (Basel, Switzerland). The reverse transcription polymerase chain reaction (RT-PCR) was performed using the Hot-StarTaq PCR kit (Qiagen), as described previously (1, 2). PCR cycling conditions were as follows: initial denaturation (15 min at 94 ° C) followed by 35 cycles of denaturation (1 min at 94 ° C), annealing (45 s at 62 ° C), and elongation (1 min at 72 ° C). After the last cycle, a final extension (7 min at 72 ° C) was added and thereafter the samples were kept at 4 ° C. PCR products were electrophoresed on 2% agarose gels in Tris acetate EDTA buffer, followed by staining with ethidium bromide.
The sequences of the primers used were;
Human VEGFR-3 (Ref. 3)
forward: 5'-CCCACGCAGACATCAAGACG-3'
reverse: 5'-TGCAGAACTCCACGATCACC-3' (380bp)
Human GAPDH (Ref. 1)
forward: 5'-ATCATCCCTGCCTCTACTGG-3'
reverse: 5'-CCCTCCGACGCCTGCTTCAC-3' (188bp)

References
1. Takei Y, Kadomatsu K, Yuzawa Y*, et al.* A small interfering RNA targeting vascular endothelial growth factor as cancer therapeutics. *Cancer Res* 64: 3365-3370, 2004
2. Suzuki Y, Ito Y, Mizuno M *, et al.* Transforming growth factor-β induces vascular endothelial growth factor-C expression leading to lymphangiogenesis in rat unilateral ureteral obstruction. *Kidney Int* 81: 865-879, 2012
3. Gockel I, Moehler M, Frerichs K*, et al.* Co-expression of receptor tyrosine kinases in esophageal adenocarcinoma and squamous cell cancer. *Oncol Rep* 20: 845-850, 2008

Supplementary Figure 2

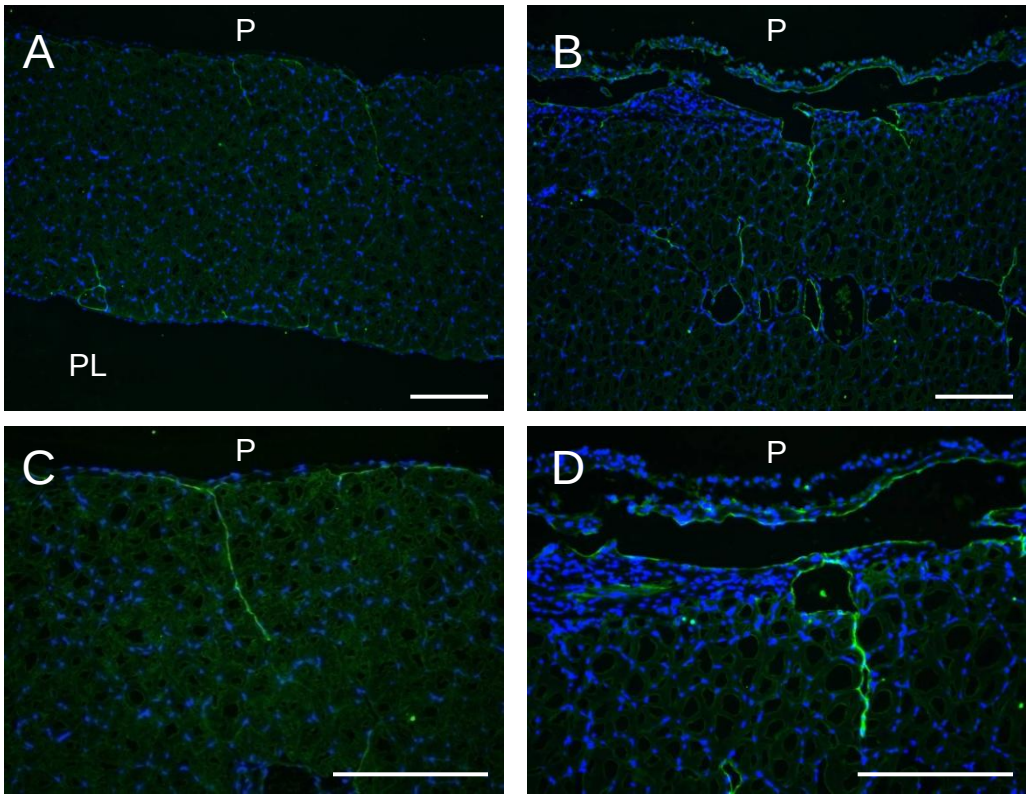

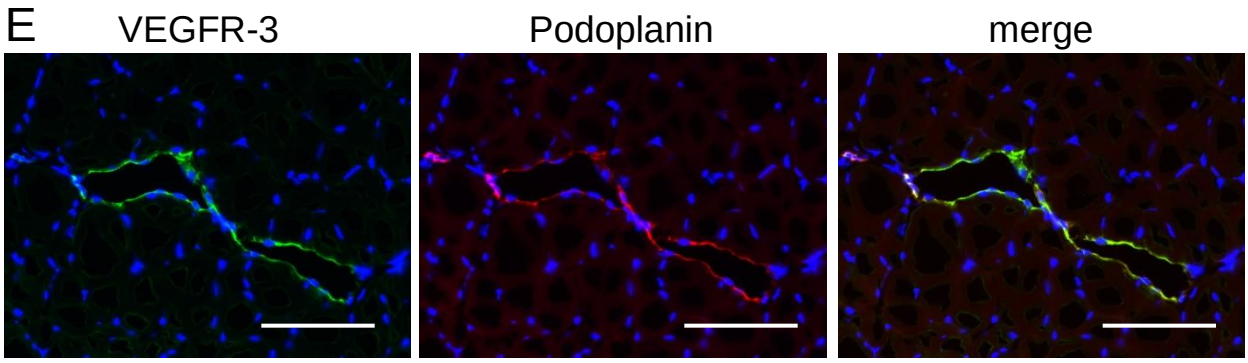

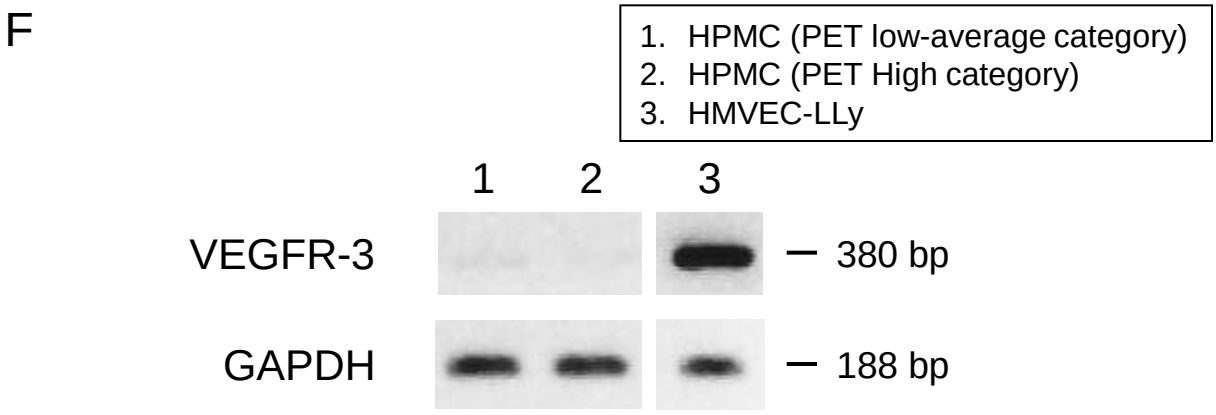

HPMC: human peritoneal mesothelial cells
HMVEC-LLy: normal human lymphatic microvasucular endothelial cells

Supplementary Figure 2

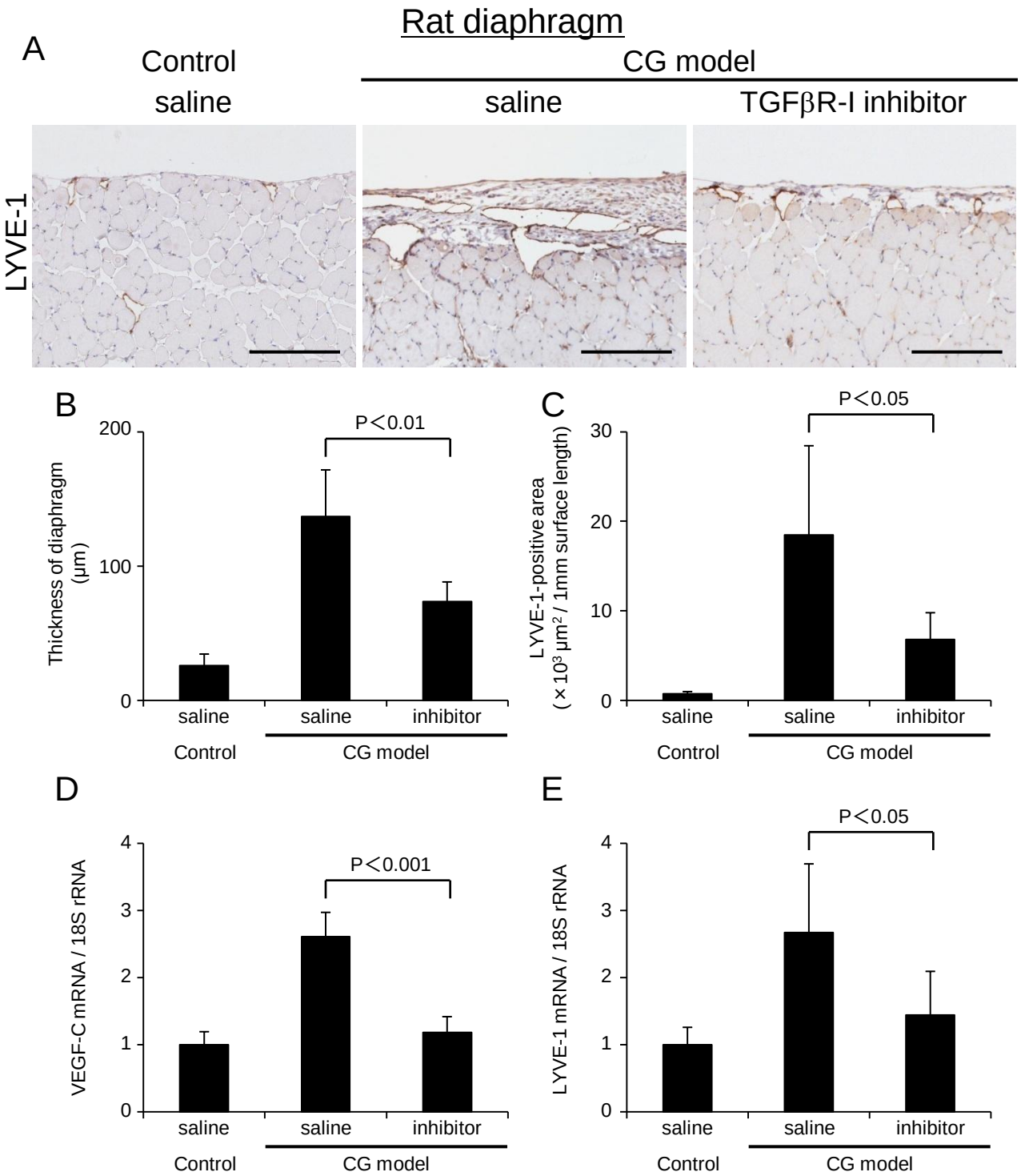

Supplementary Figure 3.
Immunohistochemical analyses, and real-time PCR analyses of selected mRNAs, in the diaphragm of TGFβR-I inhibitor-treated and untreated (saline) rats. Lymphangiogenesis was suppressed by the TGFβR-I inhibitor.

A: LYVE-1 staining of inhibitor-treated, untreated and control rats. Scale bars, 200 μm.

B: The thickness of the diaphragm was significantly reduced by TGFβR-I inhibitor treatment of CG model rats.

C: The size of the LYVE-1-positive area, as analyzed by MetaMorph, was significantly reduced by treatment with the TGFβR-I inhibitor.

D and E: The increased expression of VEGF-C and LYVE-1 mRNA in the CG model rats was suppressed by TGFβR-I inhibitor treatment.

Supplementary Figure 3

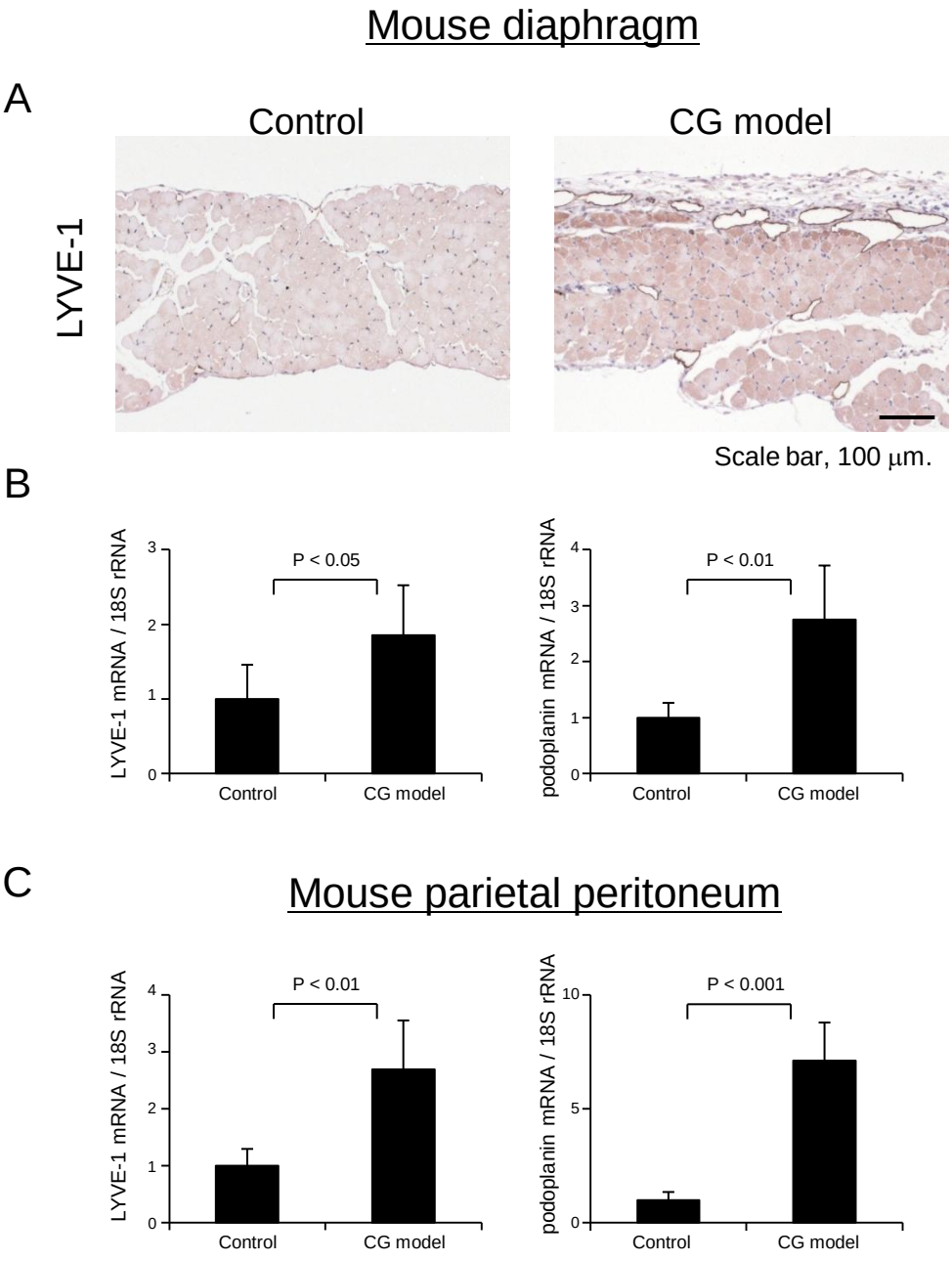

Supplementary Figure 4.
The CG model in mice is similar to that in rats. Serial section analysis showed that the lymphatic vessels were connected to the central collector of the lymphatic vessels.
Lymphangiogenesis developed in both the parietal peritoneum and diaphragm, which was similar to the rat CG model (A-C). Lymphatic vessels grown in the diaphragm were connected to the central collector of lymphatic vessels (D). Blue arrows in (D-4) of serial sections indicate the possible route of the passage for lymphatic fluid.
(A, B) mouse diaphragm; (C) mouse parietal peritoneum.

Supplementary Figure 4

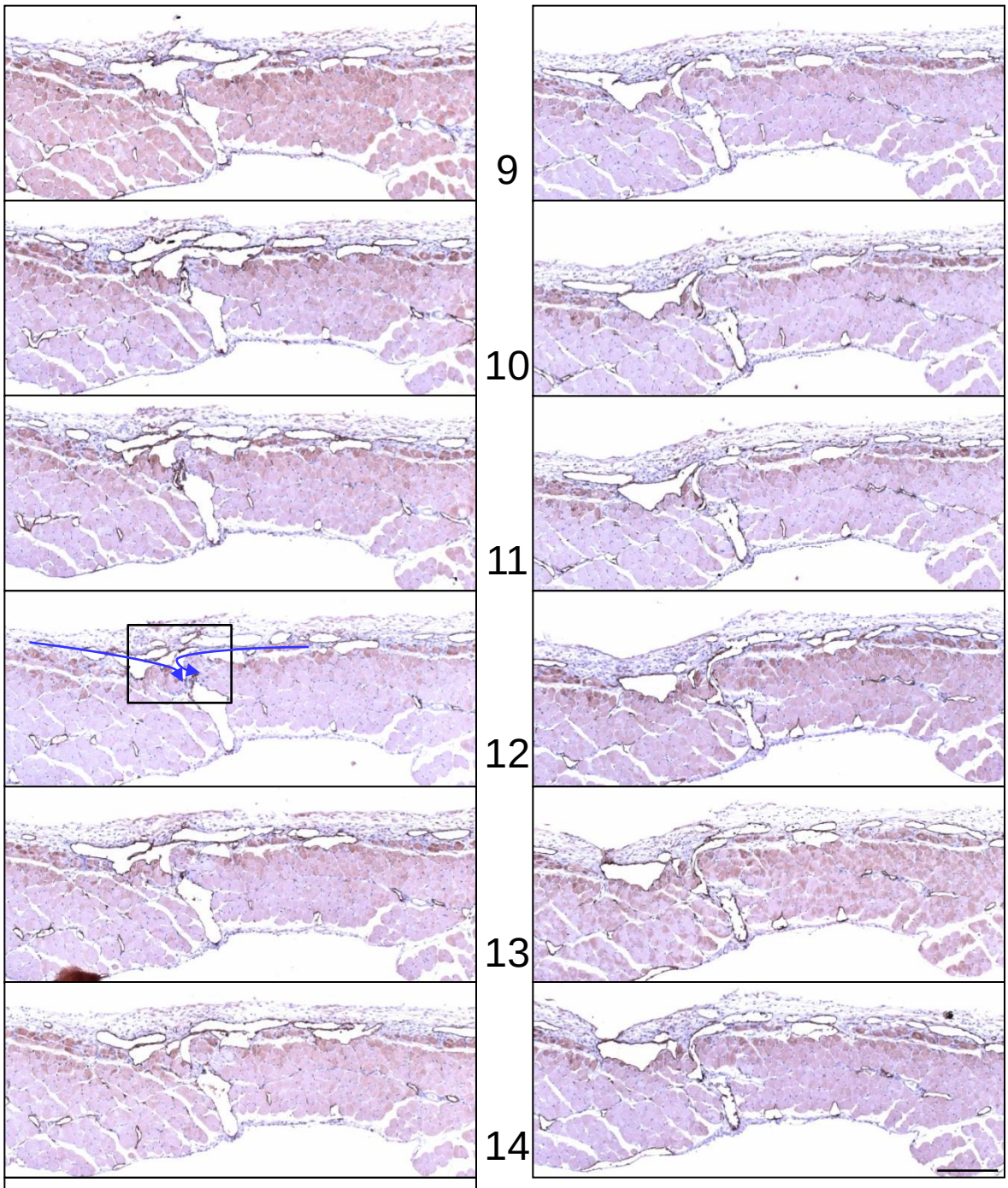

Scale bar, 200 μm.

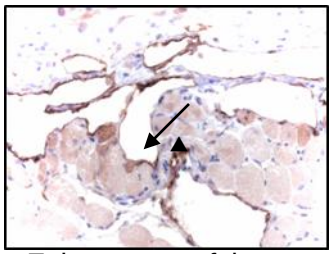

Enlargement of the rectangular frame of Fig. 4D-4.
Arrow: central collector of lymphatic vessel
Arrowhead: artery

Supplementary Figure 4 D

Supplementary Figure 5.
Newly synthesized lymphatic vessels with entrance were revealed in the diaphragm.
On analysis of the serial sections, newly synthesized lymphatic vessels with entrance (red arrows) were revealed in the fibrotic diaphragm. Black arrows indicate the edges or surroundings of the entrance of the lymphatic vessels.
* (in 4-6) and ▲(in 13-16) indicate the connections of newly synthesized lymphatic vessel system.

Supplementary Figure 5

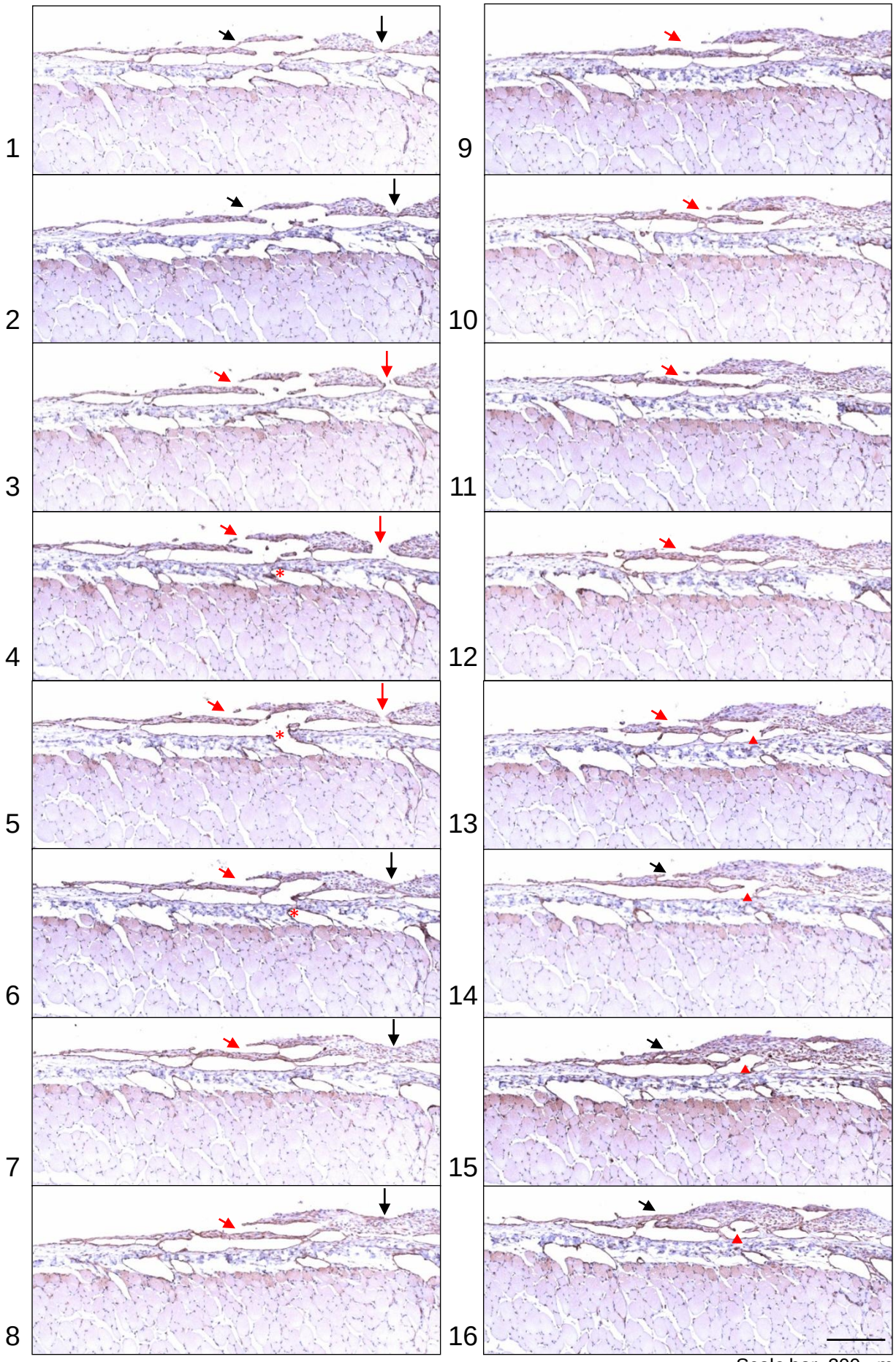

Supplementary Figure 5

Scale bar, 200 μm.

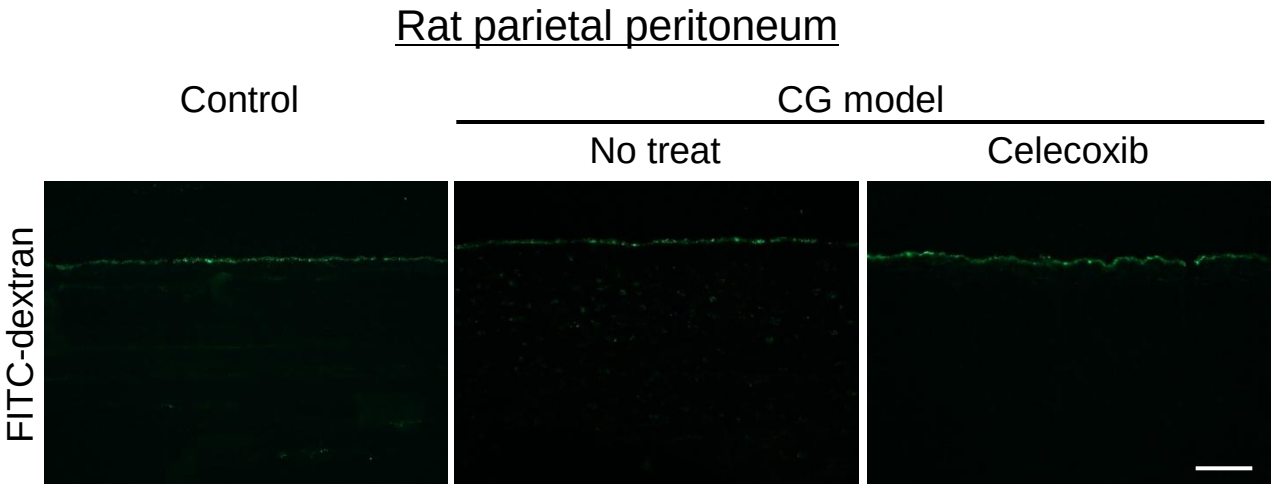

Supplementary Figure 6.
There was barely detectable FITC-dextran in the parietal peritoneum, except on the surface of the peritoneum, as seen by immunofluorescence microscopy after administration of 50 mg FITC-dextran intraperitoneally.
Left panel: control.
Middle panel: CG model with no treatment
Right panel: CG model treated with COX-2 inhibitor, Celecoxib
Scale bar, 100 μm.

Supplementary Figure 6

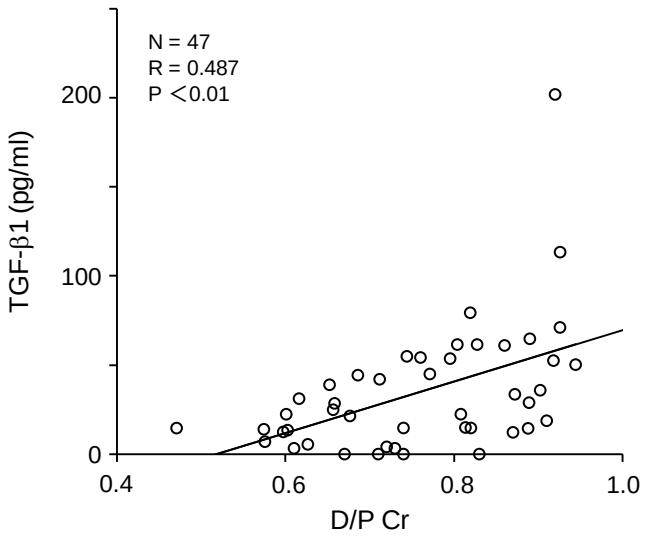

Supplementary Figure 7.

The concentration of TGF-β1 protein in human PD effluent was correlated with D/P Cr. There was a positive correlation between TGF-β1 concentration in the PD effluent of 4-h-dwelled
samples and D/P Cr.

Supplementary Figure 7

Supplementary Table 1.
List of the antibodies used

Antibody	company
mouse anti-PAL-E antibody	Abcam, Cambridge, UK
rabbit anti-human LYVE-1 antibody	Acris Antibodies GmbH, Hiddenhausen, Germany
rabbit anti-mouse LYVE-1 antibody	Acris Antibodies GmbH, Herford, Germany
rabbit anti-VEGF-C antibody	Zymed Laboratories, South San Francisco, CA
mouse anti-cytokeratin antibody	Dako, Glostrup, Denmark
mouse anti-CD68 antibody	Dako, Glostrup, Denmark
mouse anti-rat podoplanin antibody	Relia Tech GmbH, Braunschweig, Germany
goat anti-VEGFR3 (Flt-4) antibody	R&D System, Minneapolis, MN
mouse anti-rat monocyte/macrophage antibody (ED1)	BMA Biomedicals AG, Augst, Switzerland
rabbit anti-type III collagen antibody	LSL, Nagahama, Japan
mouse anti α-SMA antibody (1A4)	Dako, Glostrup, Denmark
rabbit anti-TGF-β1 antibody	Techne, Minneapolis, MN
FITC-labeled rabbit anti-mouse IgG	Invitrogen, Camarillo, CA
FITC-labeled goat anti-rabbit IgG	Invitrogen, Camarillo, CA
FITC-labeled rabbit anti-goat IgG	Sigma, Saint Louis, Missouri, USA
rhodamine labeled goat anti-rabbit IgG	Chemicon, Billerica, MA
rhodamine labeled rabbit anti-mouse IgG	Zymed Laboratories, Carlsbad, CA
DAPI (diamidino-2-phenylindole)	Sigma-Aldrich, St. Louis, MO

Supplementary Table 2.
Primers used for real-time PCR (TaqMan Gene Expression Assays)

	Assay identification number
human VEGF-C	Hs00153458_m1
human LYVE-1	Hs00272659_m1
human podoplanin	Hs00366764_m1
rat TGF-β1	Rn00572010_m1
rat VEGF-C	Rn00586458_m1
rat LYVE-1	Rn01510422_m1
rat podoplanin	Rn00571195_m1
rat VEGFR3	Rn00586429_m1
rat type III collagen	Rn01437683_m1
18S ribosomal RNA	4319413E